MULTIBODY DYNAMICS 2009, ECCOMAS Thematic Conference
K. Arczewski, J. Frączek, M. Wojtyra (eds.)
Warsaw, Poland, 29 June–2 July 2009

MODELING AND CONTROL OF PINCHING 2D OBJECT WITH ARBITRARY SHAPE BY A PAIR OF ROBOT FINGERS UNDER ROLLING CONSTRAINTS

Morio Yoshida[⋆], **Suguru Arimoto**[⋆†] **and Kenji Tahara**[‡⋆]

[⋆]RIKEN-TRI Collaboration Center, RIKEN
Nagoya, Aichi, 463-0003, Japan
e-mail: `yoshida@nagoya.riken.jp`,
web page: `http://rtc.nagoya.riken.jp/control/yoshida/index_english.html`

[†]Department of Robotics, Ritsumeikan University
Kusatsu, Shiga, 525-8577, Japan
e-mails: `arimoto@fc.ritsumei.ac.jp`

[‡]Organization for the Promotion of Advanced Research, Kyushu University
Fukuoka, 819-0395, Japan
e-mails: `tahara@ieee.org`

Keywords: Robot Finger, Rolling Contact, Arbitrary Shape, Cooperative Control, Numerical Simulation

Abstract. *Modeling and control of grasping an object with arbitrary shape by a pair of robot fingers with hemispherical ends in a horizontal plane are proposed in a mathematical and computational standpoint. The curvature of an object contour is variable due to the change of the contact point between the finger tip and object surface. Therefore, not only the time parameter "t" but also the arclength parameter "s" are needed to describe motion of the overall fingers-object system. It is shown that Euler-Lagrange's equation of motion of the overall fingers-object system should be accompanied with the first-order differential equation of arclength parameter "s", which traces out the object contour and at the same time the finger-tip circle. A control input, which is of the same category as the control input called "blind grasping", is proposed to stabilize rotational motion of the object. The control input does neither use the kinematics information of the object nor any external sensing. Finally numerical simulations evaluate the effectiveness of the proposed model and control input.*

1 INTRODUCTION

Hands have a lot of interesting properties such as redundant joint structure, soft material of a fingertip, and rolling contact. Humans easily pinch an object without considering the object shape. These facts have attracted many robotics researchers to analyze, model, control, and create robot hands Refs.[1] and [2]. However, most researches in robotics remain in kinematics or motion planning, centering the realization of force/torque closure for a stable grasp in a static sense. Rolling geometry between two objects with arbitrary shape was strictly discussed Ref.[3]. The research, however, remains in kinematic or semi-dynamic meaning. On the other hand, researchers in multibody dynamics have presented many models with constraints Refs.[4] and [5] without modeling physical interaction between a robot finger and an object with arbitrary shape even in a two-dimensional case. In fact, modeling of pinching with rolling contact that can take account of arbitrariness of the object shape has not yet been tackled.

Arimoto $et\ al.$ Ref[6], around the year of 2000, first proposed a dynamic pinching model by a pair of robot fingers with hemispherical ends under rolling constraints when the shape of a pinched object is limited to flat surfaces. Stability of motion of the overall fingers-object system called "Stability on a manifold" is rigorously discussed in a mathematical sense since rolling constraints are reflected into the dynamics of the object as wrench vectors. The redundancy resdution problem of pinching by means of a pair of fingers with redundant joints for a required task is resolved in a local sense by applying the stability concept on an equilibrium manifold. The control strategy based on index finger-thumb opposability for stabilizing motion of the overall system, which is called "blind grasping", is proposed Ref.[7], which does neither need object kinematic information nor need external sensing. The pinching model was extended in 2006 to a three-dimensional case Ref.[7]. A mathematical model is derived as a set of equations of motion of the fingers-object system under Pfaffian constraints due to rolling constraints and differential equations representing infinitesimal rotations of the pinched object. The shape of the 3D pinched object, however, has been restricted to flat surfaces.

In this paper, a new dynamical system with physical interaction, which expresses motion of pinching a 2D object with arbitrary shape by a pair of robot fingers with hemispherical ends (see Fig.1), is proposed and modeled in a mathematical and computational manner. The curvature

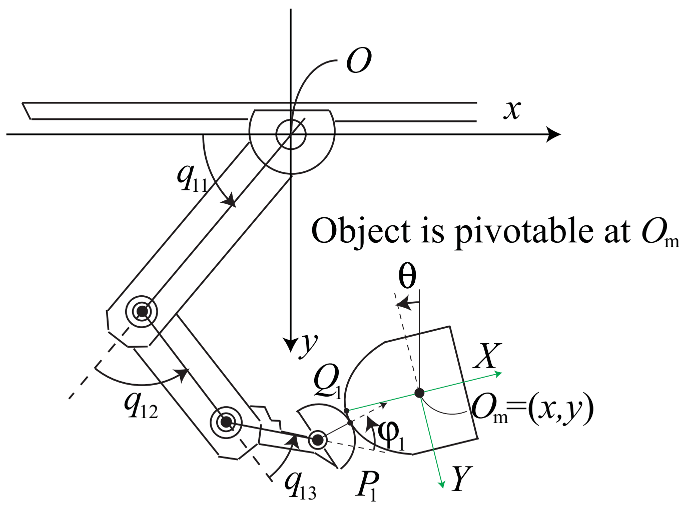

Figure 1: A three-DOF finger robot manipulating a 2-D object pivoted at a fixed point

of the object contour is variable according to the change of the contact point between the object surface and the rigid finger tip. Therefore the fingers-object dynamic equations, which should be accompanied with the update equation of arclength parameter “s”, are derived. A class of control signals called “blind grasping” is proposed for realizing stable grasping, without referring to object kinematics or using external sensing. It should be noted that the control signal is of the same as that in the case treating an object with flat surfaces Ref.[7]. In the case of one robot finger, the closed dynamics is derived, and it is shown that the given equilibrium state is satisfied from the aspect of a numerical simulation. Finally numerical simulations are carried out, for confirmation of the effectiveness of our proposed model and control input by implementing the derived mathematical model of physical interaction of rolling with the aid of a constrained stabilization scheme.

2 DYNAMICS

In order to show a key role of the rolling constraint, a mechanical setup of pinching a rigid object with arbitrary shape by one robot fingers with 3 DOFs shown in Fig.1 is investigated. The finger tip is made by rigid material and is of hemispherical shape. The object is pined at a point O_m and rotates around it. In the coordinate system, numerical values of all angles are positive in counterclockwise direction. It is assumed that the xy-plane in the figure is horizontal and the effect of the gravity is ignored. We introduce the local coordinate O_m-XY fixed at the object frame, and define unit vectors $\boldsymbol{r}_X$ on the X axis and $\boldsymbol{r}_Y$ on the Y axis (see Fig.2). The left-side contour of the object is expressed by a curve attached to the local coordinate $(X(s_1), Y(s_1))$ by virtue of an arclength parameter s_1 (see Fig.3). P_1 is the contact point between the finger tip and object surface, and $\boldsymbol{n}_1$ the normal unit vector to the tangent vector $\boldsymbol{b}_1$. The angle between the vector $\boldsymbol{n}_1$ and X axis expressed by θ_1 is determined as follows:

$$\theta_1(s_1) = \mathrm{arc}\,(X'(s_1)/Y'(s_1)) \tag{1}$$

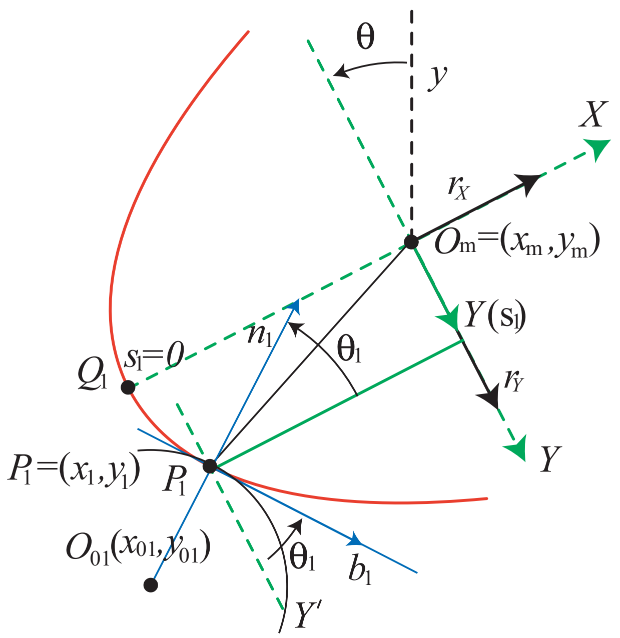

Figure 2: Relationship between local coordinate O-XY and fingertip O_{01}

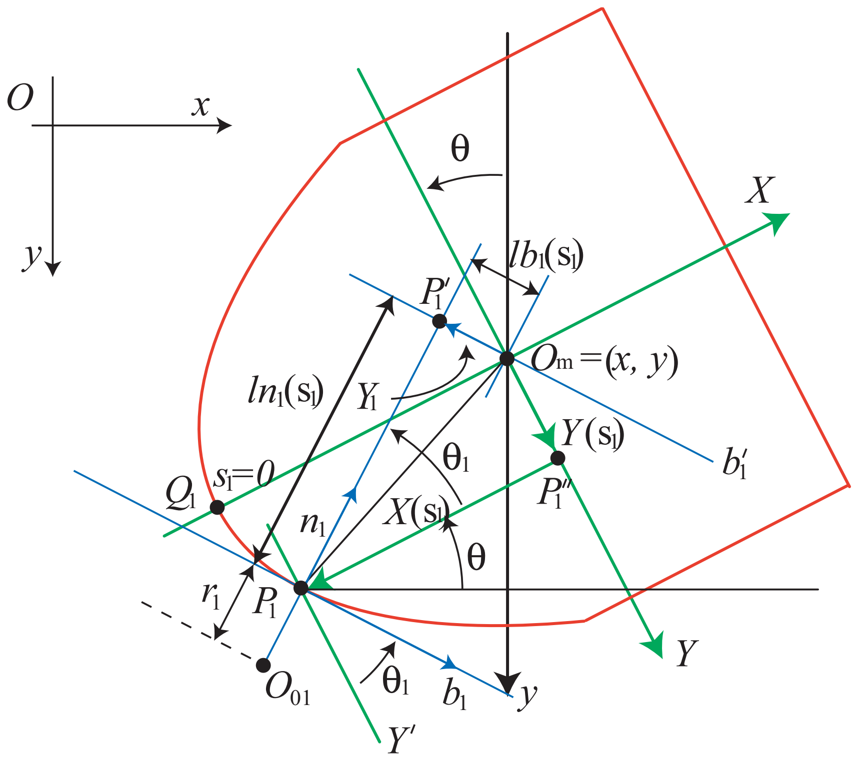

Figure 3: Geometrical relationship based on length parameter "s_1"

where $X'(s_1) = \mathrm{d}X(s_1)/\mathrm{d}s_1$ and $Y'(s_1) = \mathrm{d}Y(s_1)/\mathrm{d}s_1$. $\overline{P_1P_1'}$ is expressed in the local coordinate $(X(s_1), Y(s_1))$ as follows:

$$\overline{P_1P_1'} = l_{n1}(s_1) = -X(s_1)\cos\theta_1(s_1) + Y(s_1)\sin\theta_1(s_1) \tag{2}$$

In contrast, $\overline{P_1P_1'}$ is expressed in the inertia frame O-xy as follows:

$$\overline{P_1P_1'} = (x - x_{01})\cos(\theta + \theta_1) - (y - y_{01})\sin(\theta + \theta_1(s_1)) - r_1 \tag{3}$$

Hence, the contact constraint between the finger tip and object surface is derived as the holonomic constraint:

$$Q_1 = -(x - x_{01})\cos(\theta + \theta_1(s_1)) - (y - y_{01})\sin(\theta + \theta_1(s_1)) = -(r_1 + l_{n1}(s_1)) \tag{4}$$

$\overline{O_mP_1'}$ is expressed in the local coordinate $(X(s_1), Y(S_1))$ as follows:

$$\overline{O_mP_1'} = l_{b1}(s_1) = X(s_1)\sin\theta_1 + Y(s_1)\cos\theta_1 \tag{5}$$

On the other hand, $\overline{O_mP_1'}$ is expressed in the inertia frame as follows:

$$R_1(t) = -(x - x_{01})\sin(\theta + \theta_1) - (y - y_{01})\cos(\theta + \theta_1) = l_{b1}(s_1) \tag{6}$$

Rolling contact expresses that the robot finger tip rolls on the object surface without slipping. Thus the object's velocity along the vector $\boldsymbol{b}_1$ at the contact point P_1 must be equal to the finger tip's velocity along the vector $\boldsymbol{b}_1$ at the point, at instant t, as follows:

$$r_1\frac{\partial\phi_1}{\partial t} + \frac{\partial}{\partial t}R_1(t) = 0 \tag{7}$$

where φ_1 is defined as follows (see Fig.1):

$$\begin{aligned}\varphi_1 &= \pi + (\theta + \theta_1) - (q_{11} + q_{12} + q_{13}) \\ &= \pi + (\theta + \theta_1) - p_1\end{aligned} \tag{8}$$

where $p_1 = q_{11} + q_{12} + q_{13}$. Eq.(7) can fortunately be integrated in the sense of Frobenius (see Ref.[8]). In fact, we define

$$\overline{R_1}(t, s_1) = r_1\{\theta + \theta_1(s_1) - p_1\} + s_1 + R_1 - l_{b1}(s_1), \tag{9}$$

and see that $\partial \overline{R}_1(t, s_1)/\partial t = 0$ is reduced to Eq.(7). It is found out that (see Ref.[8])

$$\frac{\mathrm{d}\overline{R}_1}{\mathrm{d}t} = \frac{\partial \overline{R}_1}{\partial t} + \frac{\partial \overline{R_1}}{\partial s_1}\frac{\mathrm{d}s_1}{\mathrm{d}t} = 0 \tag{10}$$

Then it is possible to define

$$\tilde{R}_1 = \overline{R}_1(t, s_1(t)) - \overline{R}_1(0, s_1(0)) \tag{11}$$

By associating Lagrange's multipliers f_1 and λ_1 with the constraints $Q_1 = 0$ (Eq.4) and $\tilde{R}_1 = 0$ (Eq.11) respectively, we define a Lagrangian:

$$L = \frac{1}{2}\dot{\boldsymbol{q}}_1^{\mathrm{T}} G_1 \dot{\boldsymbol{q}}_1 + \frac{1}{2} I \dot{\theta}^2 - f_1 Q_1 - \lambda \tilde{R}_1 \tag{12}$$

where $\boldsymbol{q}_1 = (q_{11}, q_{12}, q_{13})^{\mathrm{T}}$, $G_1(q_1)$ denotes the inertia matrix, and I denotes the inertia moment of the object. By applying the variational principle, the dynamic equations of the overall finer-object system are derived as follows:

$$I\ddot{\theta} - f_1 l_{b1}(s_1) - \lambda l_{n1}(s_1) = 0 \tag{13}$$

$$G_1(\boldsymbol{q}_1)\ddot{\boldsymbol{q}}_1 + \left\{\frac{1}{2}\dot{G}_1 + S_1\right\}\dot{q}_1 + f_1 J_1^{\mathrm{T}}(\boldsymbol{q}_1)\boldsymbol{n}_1(\theta)\lambda_1\left\{J_1^{\mathrm{T}}(\boldsymbol{q}_1)\boldsymbol{b}_1(\theta) - r_1\boldsymbol{e}_1\right\} = u_1 \tag{14}$$

where $\boldsymbol{e}_1 = (1, 1, 1)^{\mathrm{T}}$, $J_1^{\mathrm{T}} = \partial(x_{01},\ y_{01})/\partial q_1$,

$$\boldsymbol{n}_1(\theta) = \begin{pmatrix} \cos(\theta + \theta_1) \\ -\sin(\theta + \theta_1) \end{pmatrix},\ \boldsymbol{b}_1(\theta) = \begin{pmatrix} \sin(\theta + \theta_1) \\ \cos(\theta + \theta_1) \end{pmatrix} \tag{15}$$

and u_1 stands for the control input. Because the arclength parameter s_1 depends on the time parameter t, the parameter s_1 should be updated as follows:

$$\frac{\mathrm{d}s_1}{\mathrm{d}t} = \frac{r_1}{1 + r_1\kappa_1(s_1)}\left(\dot{p}_1 - \dot{\theta}\right) \tag{16}$$

where κ_1 denotes the curvature of the object contour at a contact as follows:

$$\kappa_1(s_1) = X''(s_1)Y'(s_1) - X'(s_1)Y''(s_1) \tag{17}$$

It should be noted that the curvature $\kappa_1(s_1)$ of the object contour appears in the update equation (Eq.(16)) but not in the overall Lagrange's equations (Eqs.(13) and (14)).

3 CONTROL SIGNAL & CLOSED LOOP DYDAMICS

In order to immobilize rotational motion of the object, rotational motion "$-f_1 l_{b1}(s_1) - \lambda_1 l_{n1}(s_1)$" must be zero. By analogy with our previous control signals called "blind grasping" Ref.[7], we introduce the control input:

$$u_1 = -c_1\dot{\boldsymbol{q}}_1 - \left(\frac{f_d}{r_1}\right) J_1^{\mathrm{T}}(\boldsymbol{q}_1)\begin{pmatrix} x_{01} - x \\ y_{01} - y \end{pmatrix} - r_1\hat{N}_1\boldsymbol{e}_1 \tag{18}$$

where

$$\hat{N}_1(t) = \gamma_1^{-1} r_1 \left(p_1(t) - p_1(0)\right) \tag{19}$$

γ_1 and c_1 are positive constants, and $p_1(0)$ an initial value of $p_1(t)$. The first term of the right hand side of Eq.(18) plays a role of damping. The second term is introduced to cease the rotational moment of the object. The third term is introduced for saving excess movements of finger joints from the initial pose. Substituting the control input (Eq.18) into the overall finger object system (Eqs.(13) and (14)) yields the following closed-loop dynamics:

$$I\ddot{\theta} - \Delta f_1 l_{b1}(s_1) - \Delta\lambda_1 l_{n1}(s_1) + S_N = 0 \tag{20}$$

$$G_1(\boldsymbol{q}_1)\ddot{\boldsymbol{q}}_1 + \left\{\frac{1}{2}\dot{G}_1 + S_1\right\}\dot{q}_1 + \Delta f_1 J_1^{\mathrm{T}}\boldsymbol{n}_1(\theta) + \Delta\lambda_1\left\{J_1^{\mathrm{T}}(\boldsymbol{q}_1)\boldsymbol{b}_1(\theta) - r_1\boldsymbol{e}_1\right\} + r_1\Delta N_1\boldsymbol{e}_1 + c_1\dot{\boldsymbol{q}}_1 = 0 \tag{21}$$

where

$$\Delta f_1 = f_1 - \frac{f_d}{r_1}\left(r_1 + l_{n1}(s_1)\right),\ \Delta\lambda_1 = \lambda_1 + \frac{f_d}{r_1} l_{b1}(s_1) \tag{22}$$

$$\Delta N_1 = \hat{N}_1 + \frac{f_d}{r_1} l_{b1}(s_1) \tag{23}$$

$$S_N = -\frac{f_d}{r_1}\left(r_1 + l_{n1}(s_1)\right) l_{b1}(s_1) + \frac{f_d}{r_1} l_{b1} l_{n1} \tag{24}$$

4 ALGORITHMC DESIGN OF THE SIMULATOR

In order to maintain the contact and rolling constraints (Eqs.(4) and (11)), it is convenient to use the "Constraint Stabilization Method"(CSM) Ref.[9]. These algebraic equations are applied to the CSM method, and the nonlinear 2-order simultaneous differential equations are obtained as follows:

$$\begin{cases} \ddot{Q}_1 + \gamma_{f1}\dot{Q}_1 + \omega_{f1} Q_1 = 0 \\ \ddot{\tilde{R}}_1 + \gamma_{\lambda 1}\dot{\tilde{R}}_1 + \omega_{\lambda 1}\tilde{R}_1 = 0 \end{cases} \tag{25}$$

where coefficiants called CSM gains should be chosen to satisfy critical damping conditions as

$$\gamma_{f1} = 2\sqrt{\omega_{f1}},\ \gamma_{\lambda 1} = 2\sqrt{\omega_{\lambda 1}} \tag{26}$$

We define

$$\begin{cases} Q_{1q1} = \frac{\partial Q_1}{\partial \boldsymbol{q}_1}, Q_{1\theta} = \frac{\partial Q_1}{\partial \theta}, Q_{1s_1} = \frac{\partial Q_1}{\partial s_1} \\ \tilde{R}_{1q1} = \frac{\partial \tilde{R}_1}{\partial \boldsymbol{q}_1}, \tilde{R}_{1\theta} = \frac{\partial \tilde{R}_1}{\partial \theta}, \tilde{R}_{1s_1} = \frac{\partial \tilde{R}_1}{\partial s_1} \end{cases} \tag{27}$$

Then, Eq.(25) is expressed as

$$Q_{1q1}^{\mathrm{T}}\ddot{\boldsymbol{q}}_1 + Q_{1\theta}\ddot{\theta} + Q_{1s1}\ddot{s}_1 + \left(\frac{\mathrm{d}Q_{1q1}}{\mathrm{d}t} + \gamma_{f1}Q_{1q1}\right)^{\mathrm{T}}\dot{\boldsymbol{q}}_1$$
$$+\left(\frac{\mathrm{d}Q_{1\theta}}{\mathrm{d}t} + \gamma_{f1}Q_{1\theta}\right)^{\mathrm{T}}\dot{\theta}_1 + \left(\frac{\mathrm{d}Q_{1s1}}{\mathrm{d}t} + \gamma_{f1}Q_{1s1}\right)^{\mathrm{T}}\dot{s}_1 + \omega_{f1}Q_1 = 0 \tag{28}$$

$$\tilde{R}_{1q1}^{\mathrm{T}}\ddot{\boldsymbol{q}}_1 + \tilde{R}_{1\theta}\ddot{\theta} + \tilde{R}_{1s1}\ddot{s}_1 + \left(\frac{\mathrm{d}\tilde{R}_{1q1}}{\mathrm{d}t} + \gamma_{\lambda 1}\tilde{R}_{1q1}\right)^{\mathrm{T}}\dot{\boldsymbol{q}}_1$$
$$+\left(\frac{\mathrm{d}\tilde{R}_{1\theta}}{\mathrm{d}t} + \gamma_{\lambda 1}\tilde{R}_{1\theta}\right)^{\mathrm{T}}\dot{\theta}_1 + \left(\frac{\mathrm{d}\tilde{R}_{1s1}}{\mathrm{d}t} + \gamma_{\lambda 1}\tilde{R}_{1s1}\right)^{\mathrm{T}}\dot{s}_1 + \omega_{\lambda 1}\tilde{R}_1 = 0 \tag{29}$$

Since the constraints Q_1 and $\tilde{R}_1$ differentiated with respect to s_1 fortunately become zero Ref.[8], that is, $Q_{1s1} = 0$ and $\tilde{R}_{1s1} = 0$, the Equations (28) and (29) are reduced to

$$Q_{1q1}^{\mathrm{T}}\ddot{\boldsymbol{q}}_1 + Q_{1\theta}\ddot{\theta} + \left(\frac{\mathrm{d}Q_{1q1}}{\mathrm{d}t} + \gamma_{f1}Q_{1q1}\right)^{\mathrm{T}}\dot{\boldsymbol{q}}_1 + \left(\frac{\mathrm{d}Q_{1\theta}}{\mathrm{d}t} + \gamma_{f1}Q_{1\theta}\right)^{\mathrm{T}}\dot{\theta}_1 + \omega_{f1}Q_1 = 0 \tag{30}$$

$$\tilde{R}_{1q1}^{\mathrm{T}}\ddot{\boldsymbol{q}}_1 + \tilde{R}_{1\theta}\ddot{\theta} + \left(\frac{\mathrm{d}\tilde{R}_{1q1}}{\mathrm{d}t} + \gamma_{\lambda 1}\tilde{R}_{1q1}\right)^{\mathrm{T}}\dot{\boldsymbol{q}}_1 + \left(\frac{\mathrm{d}\tilde{R}_{1\theta}}{\mathrm{d}t} + \gamma_{\lambda 1}\tilde{R}_{1\theta}\right)^{\mathrm{T}}\dot{\theta}_1 + \omega_{\lambda 1}\tilde{R}_1 = 0 \tag{31}$$

where

$$\frac{\mathrm{d}Q_{1q1}}{\mathrm{d}t} = \frac{\partial Q_{1q1}}{\partial \boldsymbol{q}_1}\dot{\boldsymbol{q}}_1 + \frac{\partial Q_{1q1}}{\partial \theta}\dot{\theta}_1 + \frac{\partial Q_{1q1}}{\partial s_1}\dot{s}_1 \tag{32}$$

$$\frac{\mathrm{d}Q_{\theta}}{\mathrm{d}t} = \frac{\partial Q_{\theta}}{\partial \boldsymbol{q}_1}\dot{\boldsymbol{q}}_1 + \frac{\partial Q_{\theta}}{\partial \theta}\dot{\theta}_1 + \frac{\partial Q_{\theta}}{\partial s_1}\dot{s}_1 \tag{33}$$

$$\frac{\mathrm{d}\tilde{R}_{1q1}}{\mathrm{d}t} = \frac{\partial \tilde{R}_{1q1}}{\partial \boldsymbol{q}_1}\dot{\boldsymbol{q}}_1 + \frac{\partial \tilde{R}_{1q1}}{\partial \theta}\dot{\theta}_1 + \frac{\partial \tilde{R}_{1q1}}{\partial s_1}\dot{s}_1 \tag{34}$$

$$\frac{\mathrm{d}\tilde{R}_{\theta}}{\mathrm{d}t} = \frac{\partial \tilde{R}_{\theta}}{\partial \boldsymbol{q}_1}\dot{\boldsymbol{q}}_1 + \frac{\partial \tilde{R}_{\theta}}{\partial \theta}\dot{\theta}_1 + \frac{\partial \tilde{R}_{\theta}}{\partial s_1}\dot{s}_1 \tag{35}$$

It is important to note that $\dot{s}_1$ is obtained by the update equation of arclength parameter s_1 (Eq.(16)). By virtue of these equations (Eqs.(30) and (31)) including the object shape parameters s_1 and $\dot{s}_1$, dynamics of the overall finger-object system under the constraints composed of Eqs.(13), (14), (30), and (31) can be expressed as

$$\begin{pmatrix} G_1 & 0 & Q_{1q_1} & \tilde{R}_{1q_1} \\ 0 & I & Q_{1\theta} & \tilde{R}_{1\theta} \\ Q_{1q_1} & Q_{1\theta} & 0 & 0 \\ \tilde{R}_{1q_1} & \tilde{R}_{1\theta} & 0 & 0 \end{pmatrix} \begin{pmatrix} \ddot{\boldsymbol{q}}_1 \\ \ddot{\theta} \\ f_1 \\ \lambda_1 \end{pmatrix} = \begin{pmatrix} \boldsymbol{h}_1 \\ h_2 \\ h_3 \\ h_4 \end{pmatrix} \tag{36}$$

where

$$\begin{cases} \boldsymbol{h}_1 = u_1 - \left\{\frac{1}{2}\dot{G}_1 + S_1\right\}\dot{\boldsymbol{q}}_1 \\ h_2 = 0 \\ h_3 = -\left\{\left(\frac{\mathrm{d}Q_{1q1}}{\mathrm{d}t} + \gamma_{f1}Q_{1q1}\right)^{\mathrm{T}}\dot{\boldsymbol{q}}_1 + \left(\frac{\mathrm{d}Q_{1\theta}}{\mathrm{d}t} + \gamma_{f1}Q_{1\theta}\right)^{\mathrm{T}}\dot{\theta}_1 + \omega_{f1}Q_1\right\} \\ h_4 = -\left\{\left(\frac{\mathrm{d}\tilde{R}_{1q1}}{\mathrm{d}t} + \gamma_{\lambda 1}\tilde{R}_{1q1}\right)^{\mathrm{T}}\dot{\boldsymbol{q}}_1 + \left(\frac{\mathrm{d}\tilde{R}_{1\theta}}{\mathrm{d}t} + \gamma_{\lambda 1}\tilde{R}_{1\theta}\right)^{\mathrm{T}}\dot{\theta}_1 + \omega_{\lambda 1}\tilde{R}_1\right\} \end{cases} \tag{37}$$

The 2nd-order 6-simultaneous differential equations (eq.(36)) and first-order differential equation of arclength parameter “s_1” (eq.(16)) should be solved simultaneously so that they satisfy the principle of causality. A Runge-Kutta method can be applied to solve this differential system. The matrix of Eq.(36) is nonsingular in the situation considered in Fig.1, and the inversion of it can be carried out.

5 Numerical Simulation -PART I-

A numerical simulator is constructed, as discussed the previous chapter by using physical parameters of the finger-object system given in Table 1. Numerical simulation is carried out by applying our proposed control input (Eq.18) with the parameters of control gains and CSM gains given in Table 2 to the overall finger-object system (Eqs.(13) and (14)), in order to evaluate the stability of motion of the overall system. The curves $c(s_1)$ with local coordinates

Table 1: Physical parameters of the fingers and object.

l_{11}	length	0.065 [m]
l_{12}	length	0.039 [m]
l_{13}	length	0.026 [m]
m_{11}	weight	0.045 [kg]
m_{12}	weight	0.025 [kg]
m_{13}	weight	0.015 [kg]
$r_i (i = 1, 2)$	radius	0.010 [m]
L	base length	0.063 [m]
M	object weight	0.040 [kg]

Table 2: Parameters of control signals & CSM gains

f_d	internal force	1.000 [N]
c	damping coefficient	0.006 [Nms]
γ_1	regressor gain	0.001 [s^2/kg]
γ_{f1}	CSM gain	1500
$\gamma_{\lambda 1}$	CSM gain	3000
ω_{f1}	CSM gain	225.0×10^4
$\omega_{\lambda 1}$	CSM gain	900.0×10^4

$(X(s_1), Y(s_1))$ is used in the simulations is given

$$X(s_1) = -0.03 + \frac{\sqrt{1 + 4 \times 50^2 \times s_1^2}}{2 \times 50} \tag{38}$$

$$Y(s_1) = \frac{\mathrm{Asinh}(2 \times 50 \times s_1)}{2 \times 50} \tag{39}$$

It is noted that, because s_1 is the arclength parameter, $\sqrt{X'(s_1)^2 + Y'(s_1)^2} = 1$. The initial values of the simulation must be chosen to satisfy the rolling and contact conditions for execution of the simulation. The motion obtained by the simulation is depicted in Fig.4. If the closed-loop dynamics Eqs.(20) and (21) converge to the equilibrium state, it should satisfy

$$\ddot{\boldsymbol{q}}_1 \to 0,\ \ddot{\theta} \to 0, \dot{\boldsymbol{q}}_1 \to 0,\ \dot{\theta} \to 0,\ -\Delta f_1 l_{b1}(s_1) - \Delta\lambda_1 l_{n1}(s_1) + S_N \to 0, \tag{40}$$

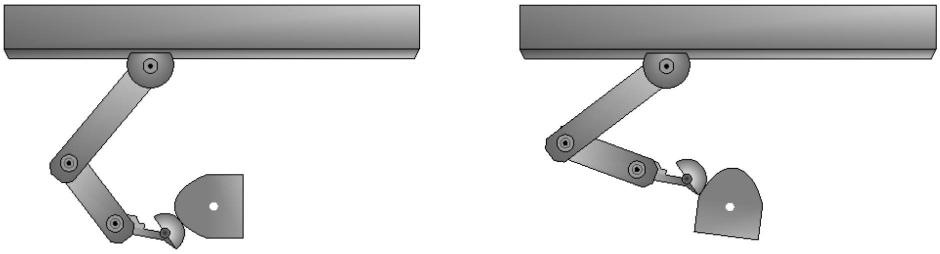

(a) Initial pose (b) After 5 seconds

Figure 4: Motion of pinching a 2-D object with arbitrary shape by one robot finger

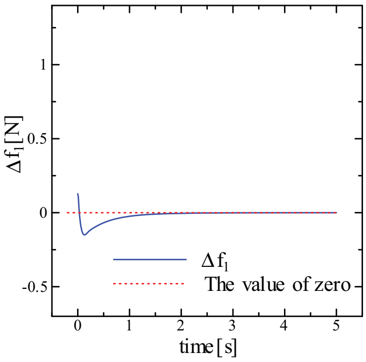

Figure 5: Δf_1

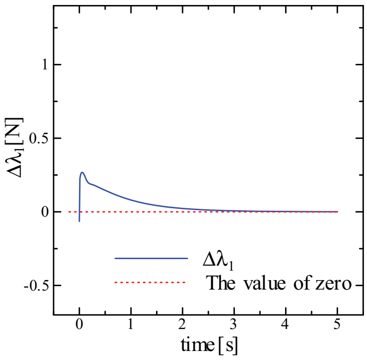

Figure 6: $\Delta\lambda_1$

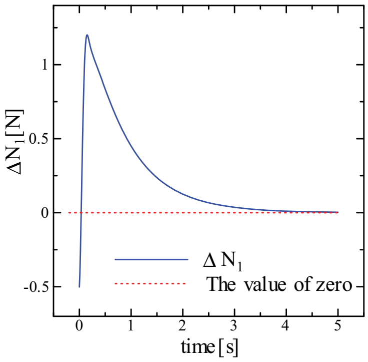

Figure 7: ΔN_1

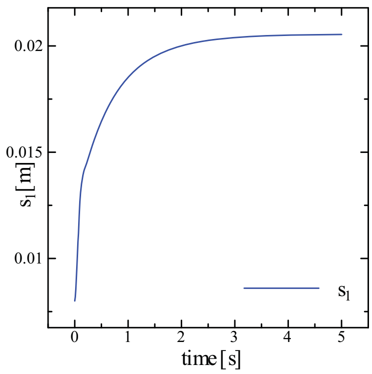

Figure 8: s_1

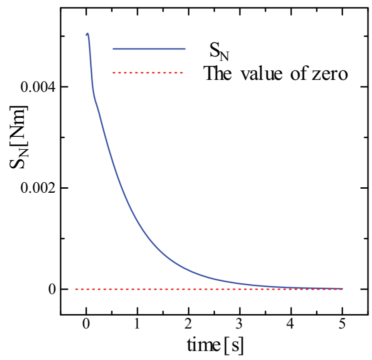

Figure 9: S_N

$$\Delta f_1 J_1^{\mathrm{T}} \boldsymbol{n}_1(\theta) + \Delta\lambda_1 \left\{ J_1^{\mathrm{T}}(\boldsymbol{q}_1)\boldsymbol{b}_1(\theta) - r_1 \boldsymbol{e}_1 \right\} + r_1 \Delta N_1 \boldsymbol{e}_1 \rightarrow 0, \ as \ t \rightarrow \infty \tag{41}$$

In fact, we confirm $\Delta f_1 \rightarrow 0$, $\Delta\lambda_1 \rightarrow 0$, ΔN_1, and $S_N \rightarrow 0$, which mean the convergence to the equilibrium state (Eqs. (40) and (41)) to some extent of satisfaction as shown in Figs 5 $\sim$ 9. The stable grasping is confirmed from the results of numerical simulation.

6 DYNAMICS -PART II-

In this section, the modeling and control proposed by the previous sections are extended to the stability problem of pinching an object by a pair of robot fingers. Similarly to θ_1 (Eq.(1)), θ_2 (see Figs.11 and 12) is determined as follows:

$$\theta_2(s_2) = \mathrm{arct}\left(X'(s_2)/Y'(s_2)\right) \tag{42}$$

where $X'(s_2) = \mathrm{d}X(s_2)/\mathrm{d}s_1$ and $Y'(s_2) = \mathrm{d}Y(s_2)/\mathrm{d}s_2$. Similarly, the contact constraint of the left side of the object is derived as the holonomic constraint:

$$Q_2 \;=\; (x - x_{02})\cos(\theta + \theta_2(s_2)) - (y - y_{02}\sin(\theta + \theta_2(s_2))) = -(r_2 + l_{n2}(s_2)) \tag{43}$$

where

$$l_{n2}(s_2) \;=\; X(s_2)\cos\theta_2(s_2) - Y(s_2)\sin\theta_2(s_2) \tag{44}$$

In a similar way, the rolling constraint at the right hand finger is derived as follows:

$$r_2\frac{\partial \phi_2}{\partial t} + \frac{\partial}{\partial t}R_2(t) = 0 \tag{45}$$

where

$$R_2(t) = -(x - x_{02})\sin(\theta + \theta_2(s_2)) - (y - y_{02})\cos(\theta + \theta_2(s_2)) = l_{b2}(s_2) \tag{46}$$

$$l_{b2}(s_2) \;=\; X(s_2)\sin\theta_2(s_2) + Y(s_2)\cos\theta_2 \tag{47}$$

$$\begin{aligned}\varphi_2 &= -\pi + (\theta + \theta_2) - (q_{21} + q_{22}) \\ &= -\pi + (\theta + \theta_2) - p_2\end{aligned} \tag{48}$$

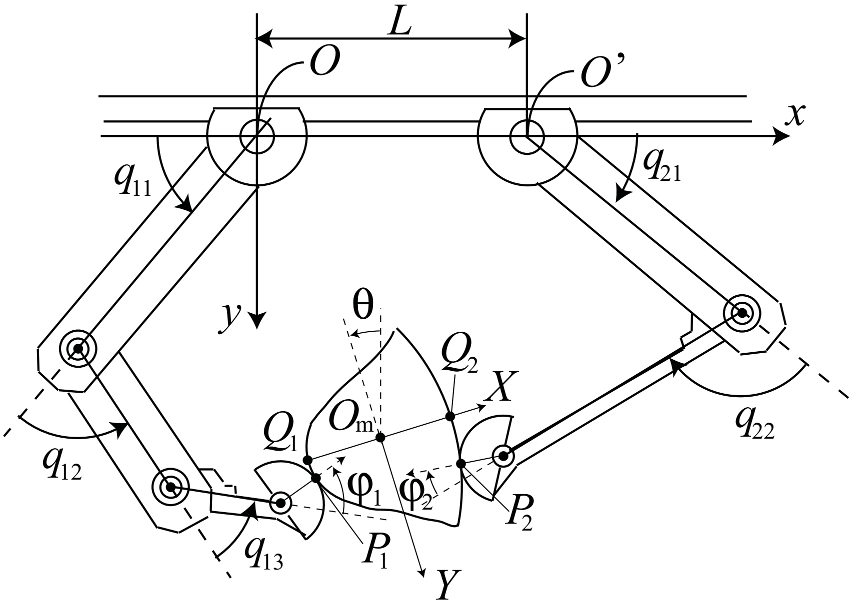

Figure 10: A pair of robot fingers grasping an object with arbitrary shape

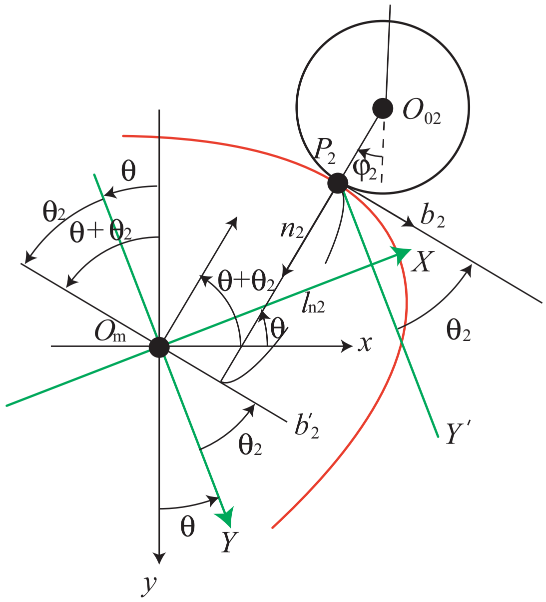

Figure 11: Geometrical relationship of the right side of an object

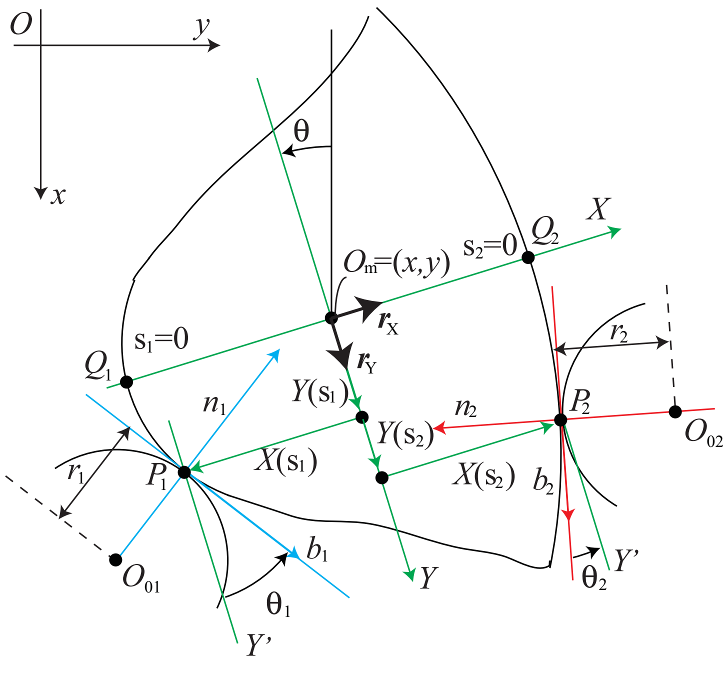

Figure 12: Relationship between fingertips O_{01} and O_{02}, and local coordinate O-XY

and $p_2 = q_{21} + q_{22}$. Equation (45) can be integrated as discussed in Eq.(7) (see Ref.[8]). Similarly we difine

$$\tilde{R}_2 = \overline{R}_2(t, s_2(t)) - \overline{R}_2(0, s_2(0)) \tag{49}$$

where

$$\overline{R_2}(t, s_2) = -r_2\{\theta + \theta_2(s_2) - p_2\} + s_2 + R_2 - l_{b2}(s_2) \tag{50}$$

and $\partial \overline{R}_2(t, s_2)/\partial t = 0$ leads to Eq.(45). It is possible to confirm the following (see Ref.[8]):

$$\frac{\mathrm{d}\overline{R}_2}{\mathrm{d}t} = \frac{\partial \overline{R}_2}{\partial t} + \frac{\partial \overline{R}_2}{\partial s_2}\frac{\mathrm{d}s_2}{\mathrm{d}t} = 0 \tag{51}$$

By associating Lagrange's multipliers f_i and λ_i $(i = 1, 2)$ with the constraints Q_i and $\tilde{R}_i$ $(i = 1, 2)$ respectively, we define a Lagrangian:

$$L = \sum_{i=1,2} \frac{1}{2}\dot{q}_i^{\mathrm{T}} G_i(q_i)\dot{\boldsymbol{q}}_i + \frac{1}{2}M(\dot{x}^2 + \dot{y}^2) + \frac{1}{2}I\dot{\theta}^2 - \lambda_1\tilde{R}_1 - \lambda_2\tilde{R}_2 - f_1Q_1 - f_2Q_2 \tag{52}$$

where $\boldsymbol{q}_2 = (q_{21}, q_{22})^{\mathrm{T}}$, $G_2(\boldsymbol{q}_2)$ denotes the inertia matrix for finger 2, M denotes the mass of the object. From the variational principle, the Lagrange equation of motion of the overall fingers-object system is derived:

$$G_i(\boldsymbol{q}_i)\ddot{\boldsymbol{q}}_i + \left\{\frac{1}{2}\dot{G}_i + S_i\right\}\dot{\boldsymbol{q}}_i - f_iJ_i^{\mathrm{T}}(\boldsymbol{q}_i)\boldsymbol{n}_i - \lambda_i\left\{J_i^{\mathrm{T}}(\boldsymbol{q}_i)\boldsymbol{b}_i - r_i\boldsymbol{e}_i\right\} = u_i, i = 1, 2 \tag{53}$$

$$M(\ddot{x}\ \ddot{y})^{\mathrm{T}} + f_1\boldsymbol{n}_1 + f_2\boldsymbol{n}_2 + \lambda_1\boldsymbol{b}_1 + \lambda_2\boldsymbol{b}_2 = 0 \tag{54}$$

$$I\ddot{\theta} - f_1Y_1 + f_2Y_2 + \lambda_1 l_{n1} - \lambda_2 l_{n2} = 0 \tag{55}$$

where $\boldsymbol{e}_2 = (1, 1)^{\mathrm{T}}$, $J_2^{\mathrm{T}} = \partial(x_{02},\ y_{02})/\partial q_2$,

$$\boldsymbol{n}_2(\theta) = \begin{pmatrix} \cos(\theta + \theta_2) \\ -\sin(\theta + \theta_2) \end{pmatrix},\ \boldsymbol{b}_2(\theta) = \begin{pmatrix} \sin(\theta + \theta_2) \\ \cos(\theta + \theta_2) \end{pmatrix} \tag{56}$$

Similarly the parameter s_2 should be updated as follows:

$$\frac{\mathrm{d}s_2}{\mathrm{d}t} = -\frac{r_2}{1 + r_2\kappa_2(s_2)}\left(\dot{p}_2 - \dot{\theta}\right) \tag{57}$$

where κ_2 denotes the curvature of the right side of the object contour as follows:

$$\kappa_2(s_2) = -X''(s_2)Y'(s_2) + X'(s_2)Y''(s_2) \tag{58}$$

7 Control Signal -PART II-

In this chapter, we extend our proposed control input (Eq.(18)) to the model of two robot fingers pinching an object with arbitrary shape. The control scheme is of the same category as the control input called "blind grasping" Ref.[8], which need neither use the kinematic information of the object nor use any external sensing; It is possible to stabilize the object without consideration of the difference between the two sides of the object's contour. The control input is proposed as follows:

$$u_i = -c_i\dot{\boldsymbol{q}}_i - \left(\frac{f_d}{r_1 + r_2}\right)J_i^{\mathrm{T}}(\boldsymbol{q}_i)\begin{pmatrix} x_{01} - x_{02} \\ y_{01} - y_{02} \end{pmatrix} - r_i\hat{N}_i\boldsymbol{e}_i,\ i = 1, 2 \tag{59}$$

where

$$\hat{N}_i(t) = \gamma_i^{-1}r_1\left(p_i(t) - p_i(0)\right),\ i = 1, 2 \tag{60}$$

γ_i and $c_i (i = 1, 2)$ are positive constants, and $p_i(0)$ initial values of $p_i(t)$ for $i = 1, 2$. The first and third terms are of the same meaning as Eq.(18). The second term is a signal based upon the opposable force between O_{01} and O_{02}.

8 Numerical Simulation -PART II-

The construction method of the simulator stated in the chapter 4 is extended to the model of two robot fingers shown in Fig.10. We construct a numerical simulator based on physical parameters of the fingers-object system given in Table 3. Numerical simulation is executed with

Table 3: Physical parameters of the fingers and object.

$l_{11}=l_{21}=l_{22}$	length	0.065 [m]
l_{12}	length	0.039 [m]
l_{13}	length	0.026 [m]
m_{11}	weight	0.045 [kg]
m_{12}	weight	0.025 [kg]
m_{13}	weight	0.015 [kg]
m_{21}	weight	0.045 [kg]
m_{22}	weight	0.040 [kg]
$r_i(i=1,2)$	radius	0.010 [m]
L	base length	0.063 [m]
M	object weight	0.040 [kg]

Table 4: Parameters of control signals & CSM gains

f_d	internal force	0.500 [N]
c	damping coefficient	0.006 [Nms]
$\gamma_i(i=1,2)$	regressor gain	0.001 [s^2/kg]
$\gamma_{fi}(i=1,2)$	CSM gain	1500
$\gamma_{\lambda i}(i=1,2)$	CSM gain	3000
$\omega_{fi}(i=1,2)$	CSM gain	225.0×10^4
$\omega_{\lambda i}(i=1,2)$	CSM gain	900.0×10^4

our proposed control input (Eq.59) using the parameters of control gains and CSM gains given in

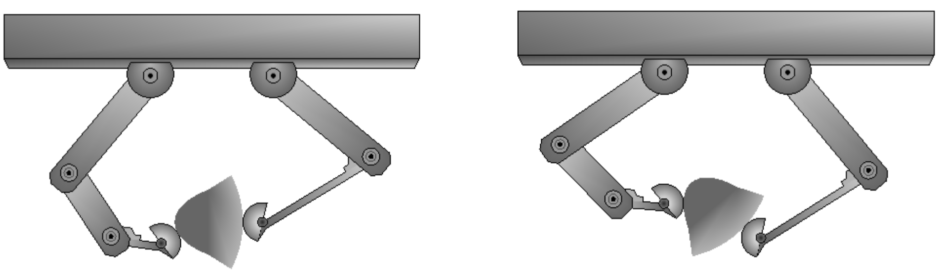

(a) Initial pose (b) After 10 seconds

Figure 13: Motion of pinching a 2-D object with arbitrary shape by a pair of robot fingers

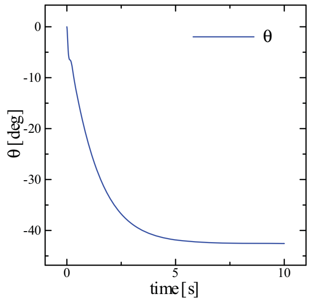

Figure 14: θ

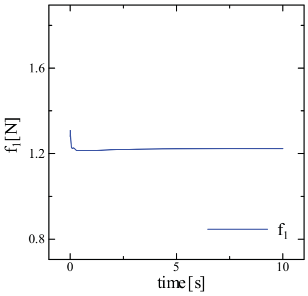

Figure 15: f_1

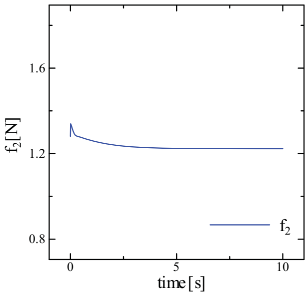

Figure 16: f_2

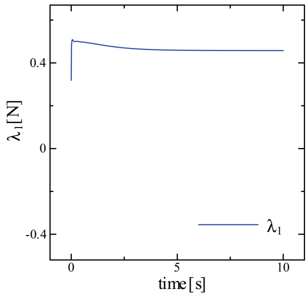

Figure 17: λ_1

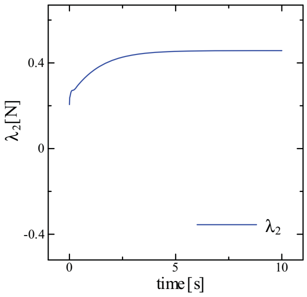

Figure 18: λ_2

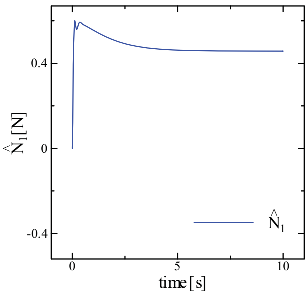

Figure 19: $\hat{N}_1$

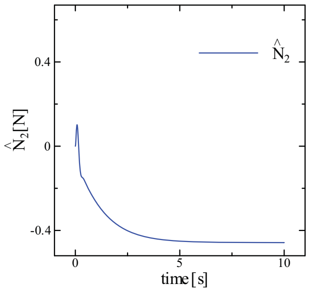

Figure 20: $\hat{N}_2$

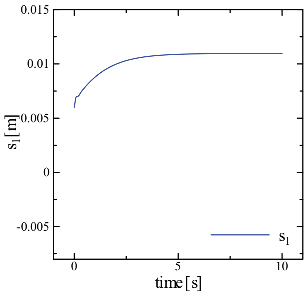

Figure 21: s_1

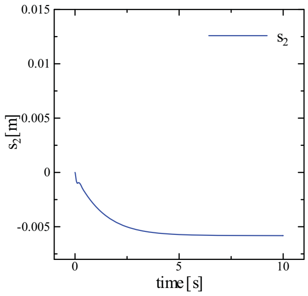

Figure 22: s_2

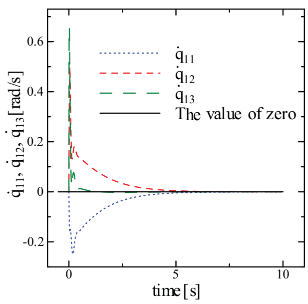

Figure 23: $\dot{q}_{11}$,$\dot{q}_{12}$ and $\dot{q}_{13}$

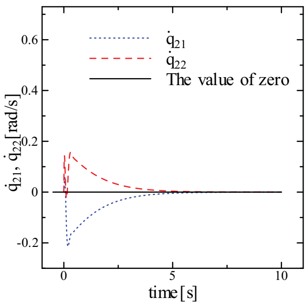

Figure 24: $\dot{q}_{21}$ and $\dot{q}_{22}$

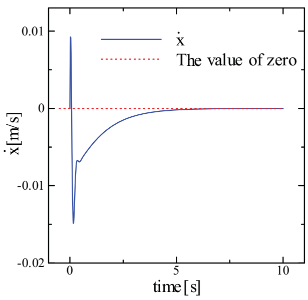

Figure 25: $\dot{x}$

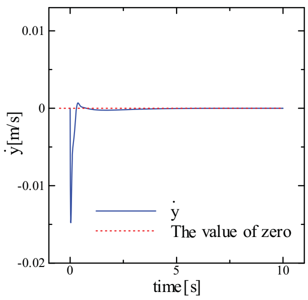

Figure 26: $\dot{y}$

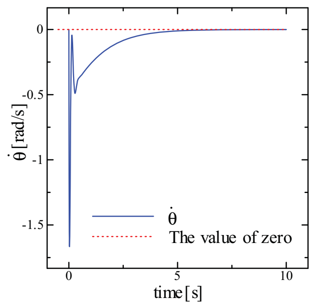

Figure 27: $\dot{\theta}$

Table 4, in order to confirm the stability of motion of the overall fingers-object system (Eqs.(53) ∼(55)). The curves $c(s_i)$,$(i{=}1,2)$ with local coordinates $(X(s_i), Y(s_i))$ in the simulations are given as follows (see Fig.11):

$$X(s_1) = -0.03 + \frac{\sqrt{1 + 4 \times 50^2 \times s_1^2}}{2 \times 50} \tag{61}$$

$$Y(s_1) = \frac{\mathrm{Asinh}(2 \times 50 \times s_1)}{2 \times 50} \tag{62}$$

$$X(s_2) = 0.065 - \frac{\sqrt{1 + 4 \times 10^2 \times s_2^2}}{2 \times 10} \tag{63}$$

$$Y(s_2) = \frac{\mathrm{Asinh}(2 \times 10 \times s_2)}{2 \times 10} \tag{64}$$

Motion of the overall fingers-object system is shown in Fig.13. The results of simulation show that all velocities of the dynamic equations (Eqs.(53) $\sim$ (55)) converge to zero, and that all Lagrange's multipliers converge to some constant values according to Figs.15 $\sim$ 18 and 23 $\sim$ 27. These results mean that motion of the overall system converges to some equilibrium state, and stable grasping is finally achieved from the viewpoint of numerical simulation.

9 CONCLUSION

In this paper, motion of the overall finger-object system with the arbitrary shape of an object is modeled in a mathematical and computational manner, and the system is extended to the mechanical setup of pinching an object by a pair of robot fingers. A control input is proposed to stabilize the object, in terms of neither the object kinematic information nor any external sensing. The control input is of the same as that in the case of handling an object with flat surfaces, despite the difference between object shapes. A design methodology of a numerical simulator is presented in our model. The proposed constraint stabilization method, including the arclength parameter "s" expressing the object posture and "$\mathrm{d}s/\mathrm{d}t$" obtained by the update equation of "s", plays the crucial role to maintain the both contact and rolling constraints, during carrying out numerical simulations. These results based on the methodology demonstrate to confirm the stability of motion of the overall system and the effectiveness of our proposed control signals.

10 ACKNOWLEDGEMENTS

This work was partially supported by Japan Society for the Promotion of Science (JSPS), Grant-in-Aid for Scientific Research (B) (20360117).

REFERENCES

[1] K. B. Shimoga. Robot grasp synthesis algorithms: A survey. *Int. J. of Robotics Research*, **15-3**, pp.230-266, 1996.

[2] B. Sicilliano and O. Khatib (eds.) *Springer Handbook of Robotics*. Springer-Verlag, New York, 2008.

[3] D.J. Montana. The kinematics of contact and grasp, *Int. J.of Robotics Research*, **7-3**, pp.17-32, 1988.

[4] T. R. Kane *Dynamics*. Holt, Rinehart and Winston, Inc, New York, 1968

[5] A.A. Shabana *Computational Dynamics, Second Edition*, Wiley-Interscience, New York, USA, 2001.

[6] S. Arimoto, P.T.A. Nguyen, H.-Y. Han, and Z. Doulgeri. Dynamics and control of a set of dual fingers with soft tips, *Robotica*, **18-11**, pp.71-80, 2000.

[7] S. Arimoto *Control Theory of Multi-fingered Hands*, Springer-Verlag, London, 2008.

[8] S. Arimoto. Dexterity and Control of Robot Arms and Hands: A Riemannian Geometry Approach, *IEICE Fundamentals Review*, **2-4**, 2009 (accepted).

[9] J. Baumgarte. Stabilization of constraint and integrals of motion in dynamical systems, *Comput. Methods in Appl. Mech. and Eng.*, **1-1**, pp.1–16, 1972.